A comparative study and overview on the magnetic resonance images skull stripping methods and their correspondence techniques

Rasha Helmi Nayyef[a], Mohammed S.H. Al-Tamimi[a,*]

[a]Department of Computer Science, College of Science, University of Baghdad, Baghdad, Iraq

(Communicated by Madjid Eshaghi Gordji)

Abstract

It is crucial to remember that the brain is a part of the body responsible for a wide range of sophisticated bodily activities. Brain imaging can be used to diagnose a wide range of brain problems, including brain tumours, strokes, paralysis, and other neurological conditions. An imaging technique known as Magnetic Resonance Imaging (MRI) is a relatively new method that can classify and categorize the brain non-brain tissues through high-resolution imaging's. For automated brain picture segmentation and analysis, the existence of these non-brain tissues is seen as a critical roadblock to success. For quantitative morphometric examinations of MR brain images, skull-stripping is often required. Skull-stripping procedures are described in this work, as well as a summary of the most recent research on skull-stripping.

Keywords: Magnetic Resonance Image, Brain, Skull-stripping, Segmentation, Convolutional Neural Network, Feature Extraction.

1. Introduction

The human brain is the body's most complex and intriguing organ. The human brain is unlike anything else on the planet in terms of intricacy, which is composed of numerous intricate neurons. As illustrated in Figure 1, this great organ regulates all bodily activities, receives and analyses information from the outside world, and embodies the essence of the mind.

---

*Corresponding author

Email addresses: rasha.helmi1986@gmail.com (Rasha Helmi Nayyef), m_altamimi75@yahoo.com (Mohammed S.H. Al-Tamimi)
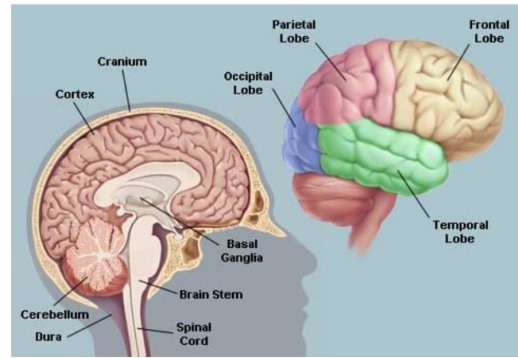
Figure 1: Overview Structure of Human Brain [6]

Numerous hazardous disorders have been uncovered that impair the brain's function. Due to the intricacy of the brain's anatomical structure, detecting such conditions is a complex undertaking. Techniques for analyzing MR brain images are frequently utilized to discover anomalies in the human brain. There are numerous high-resolution imaging techniques available today, including; MRI [3], Single-Photon Emission Tomography (SPECT), Positron Emission Tomography (PET), and Computed Tomography (CT) (see Figure 2) [16].
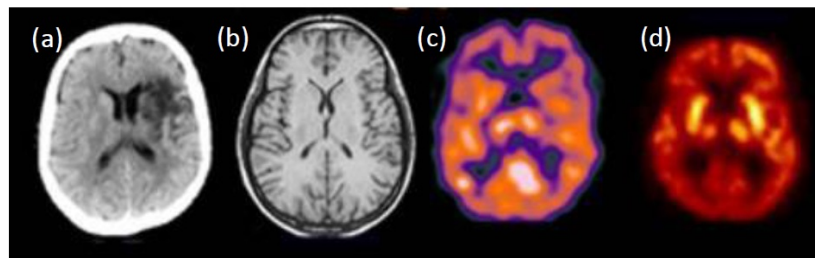
Figure 2: Human Brain Images Slices; (a) CT, (b) MRI, (c) SPET, and (d) PET [5].

The skull is the most challenging component of the human head. It works as a protective shield around the brain. The skull must be detached from the image for diagnostic purposes. In brain imaging applications, skull stripping is a vital step since it involves the removal of non-cerebral structures such as the skull, scalp, vein, and meninges [47]. Various automated and semi-automated skull stripping approaches have been developed and will be discussed in the following sections of this article.

2. MR Images Dataset Types

Due to the great interest in the topic of human brain skull stripping, the researchers worked to find many dataset, such as: (1) Clinical dataset [120, 82], (2) NeoBrainS12 [76], (3) LBPA40 [74, 12], (4) Hammers67n20 [74], (5) ABIDE [36], (6) iSeg2017 [17], (7) BrainWeb [22], (8) BLSA [65], (9) MIRIAD [68], (10) GARD [1]. Other standard data sets that were more frequent in relying on their results as described were also included in this study, which is as follows:

2.1. Brain MRI Public Dataset

Computer-Assisted Intervention (MICCAI), Open Access Series of Imaging Studies (OASIS), Medical Image Computing, Internet Brain Segmentation Repository (IBSR), and Alzheimer's Disease

Neuroimaging Initiative (ADNI) data sets are among the most commonly used for brain MRI images. The 3D cross-sectional brain MRI data evaluation framework [4], as follows:

2.1.1. OASIS Dataset

A large amount of longitudinal and cross-sectional brain MRI data from both non-demented and demented persons is managed by the Alzheimer's Disease Research Center (ADRC) at Washington University [72]. There are 416 subjects in the cross-sectional category between the ages of 18 and 96 in the longitudinal dataset, including repeated scans of each individual. Testing for Alzheimer's disease risk factors can be done with tools such as CDRs [78] and the Mini-Mental State Exam (MMSE) [93]. Figure 3 depicts the risk variables for CDR 0 (non-demented), CDR 0.5 (very mild dementia), CDR 1 (mild dementia), and CDT 2 (moderate dementia).
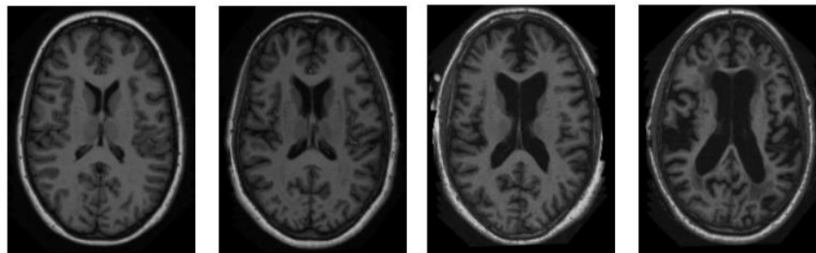
Figure 3: OASIS Data Set Sample [72]

2.1.2. ADNI Dataset

The ADNI dataset [58] contains MRI scans for 843 patients diagnosed with Alzheimer's disease in the elderly using scanning intensity fields ranging from 1.5T to 3T. The dataset includes MRI scans for 843 patients diagnosed with Alzheimer's disease in the elderly using scanning intensity fields ranging from 1.5T to 3T. Patients with Mild Cognitive Impairment are more likely to be diagnosed when their thinking and memory are affected (MCI). As illustrated in Figure 4, they also have a high probability of progressing to Alzheimer's disease (AD) or any other form of dementia. As a result, they are categorized separately from AD.
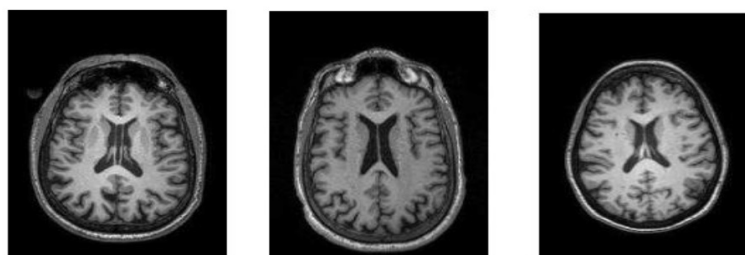
Figure 4: ADNI Data Set Sample [2]

2.1.3. IBSR Dataset

In this dataset, which includes MRI data that professionals have manually guided, IBSR [6] is used to evaluate and enhance technique evaluation. Real T1-weighted MRIs with humanly controlled expert segmentation results, known as the ground truth, are included in this collection of images. About 60 coronal T1-W segments (the distance across subsequent segments) and 18 cortical slices (the distance between successive sections) are included for each MRI volume, each with a 1.5 mm

resolution. The dimensions of $(256 \times 256 \times 128)$ pixels represent the subject volumes of this dataset with different voxel spacing's of $1.0 \times 1.0 \times 1.5mm^3$, $0.84 \times 0.84 \times 1.5mm^3$, $0.94 \times 0.94 \times 1.5mm^3$. Figure 5 depicts the noncortical structures of the Massachusetts General Hospital, which includes an additional 32 structures.
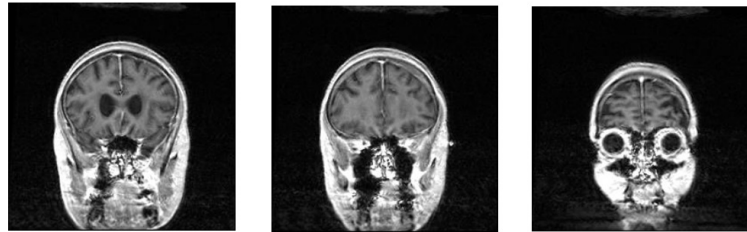
Figure 5: IBSR Data Set Sample [6]

2.1.4. MICCAI Dataset

The primary targets are 35 T1-W MRI volumes and 134 manually segmented structures in the MICCAI-2012 dataset [17] from Neuromorphometrics, Inc., Scotts Valley; CA, USA Structure, malignancy, and tissue technique. In 2012, there were 80 genuine and synthetic cases included in this data collection. Over time, the amount of training and testing data has grown. Figure 6 shows how the MICCAI 2012 challenge in multi-atlas labelling is utilized to segment sub-cortical structures.
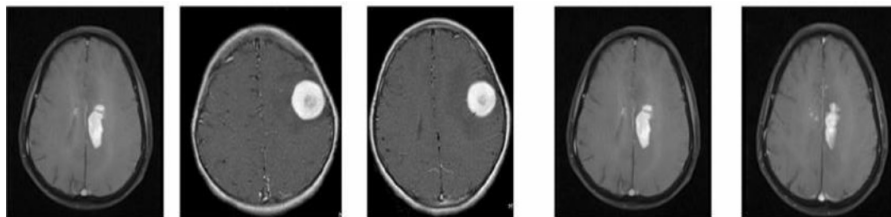
Figure 6: MICCAI Data Set Sample [17]

3. Related Literatures Analysis

Grey Matter (GM) and White Matter (WM) are the two parts of the human brain. In the brain's grey matter, the cell bodies, known as glial cells, neuropil capillaries, and synapses, represent a vital component of the central nervous system. It is a procedure that removes brain tissue by slicing open the skull. Various skull tripping methods and techniques are available in the literature, often classified as either traditional or deep learning approaches.

3.1. Conventional Methods

3.1.1. Histogram Thresholding with Mathematical Morphology

By using histogram analysis, edge detection, and other morphological procedures (e.g., elongation/dilation/opening/closing), thresholding can be used to distinguish between the brain and non-brain regions. For example, Brummer et al. [19] developed one of the most widely used approaches based on this concept. It uses histogram thresholding and mathematical morphology filters to distinguish between the skull and the brain. When Atkins and colleagues [8] segmented the brain, they
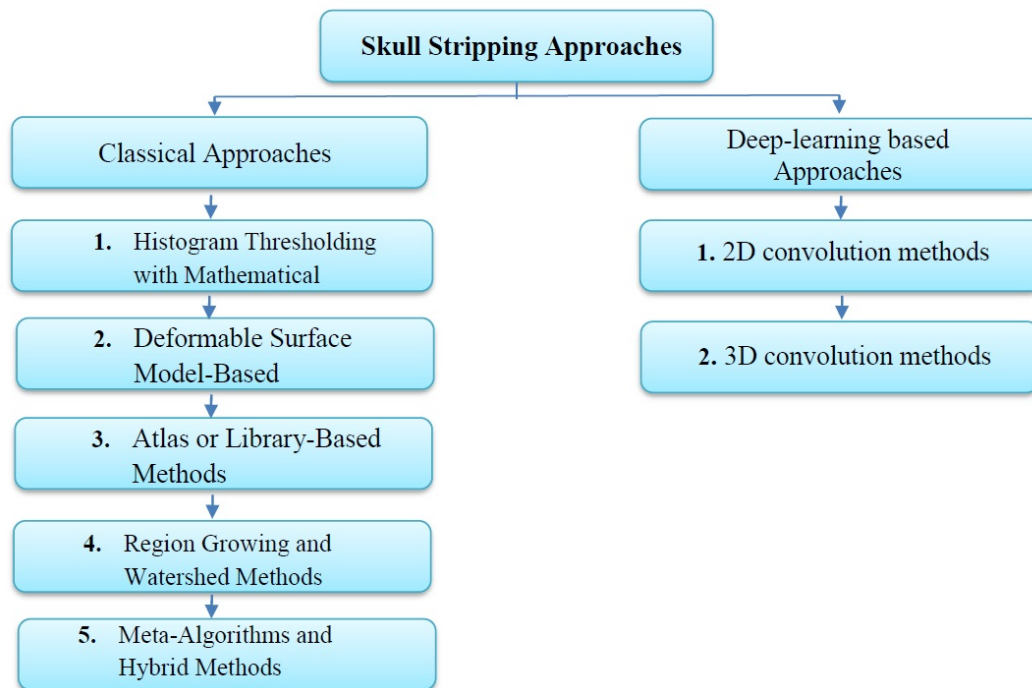
Figure 7: The flow list of the methods and techniques of Skull Stripping.

used anisotropic filters, morphology filter, histogram thresholding, and snakes contouring techniques, among other techniques.

The Histogram-Based Brain Segmentation (HBRS) approach developed by Shan et al. [98] is based on histogram and morphological procedures. Automated skull stripping using Galdames et al. [43] SMHASS (Simplex Mesh and Histogram Analysis Skull Stripping) approach was proposed by Galdames et al. First, a crude segmentation step is utilized to locate an ideal starting point for the deformation by using thresholds and morphological processes. Local grey levels and information from basic segmentation grey level modelling regulate simplex mesh deformation. Somasundaram and Kalaiselvi created the Brain Extraction Algorithm (BEA) for T1-W and T2-W brain MRI data based on diffusion, morphological techniques, and Connect Component Analysis (CCA) [106, 107]. Gambino et al. [44] suggested a two-dimensional (2D) brain extraction based on fuzzy c-means and morphological procedures.

Developed by Shattuck et al. [101], the Brain Surface Extractor (BSE) is a widely used tool for skull stripping.

Brain and non-brain regions are distinguished using a combination process of Marr-Hildreth edge detector, anisotropic diffusion filtering, and morphological detections. The BSE is incredibly rapid and produces highly detailed whole-brain segmentation, making it ideal for neuroimaging applications, which takes around 3.5 ± 0.4 seconds to retrieve the entire brain image. To allow for human interaction, the user interface provided by BSE is part of BrainSuite [99]. This method has a significant drawback in that it requires a specific brain MRI dataset to work.

As described by Somasundaram et al. [105], the greyscale transformation method utilizes morphological processes. Methods like Sadananthan et al. [94] use greyscale level thresholding and the deletion of thin connections to create a fine brain mask, like other techniques. Instead of using morphological filters, a graph section technique was examined. Balan and colleagues [11] named an automatic skull-stripping system HEAD, which is based on their findings and integrates an efficient histogram analysis procedure and binary morphological techniques (human encephalon automatic

delimiter). The Statistical Morphology Skull Stripper (SMSS), developed by Chiverton et al. [29], delineates the brain in an MRI scan by employing statistical self-similarity and morphological operations. Despite this, their approach results in a somewhat over- and under-segmentation of the brain when removing the skull. S. Roy et al. [92] developed ARoSi, a method for removing both resilient skulls and based on rough-fuzzy connectivity. Among the most current strategies are those proposed by Kavitha Srinivasan et al. [110], who has introduced mathematical morphology-based approaches that are clever and resilient [18, 115].

However, this method has the fundamental issue of requiring empirical testing to discover many of the parameters necessary to perform morphological operations, such as the forms and sizes of structural elements. There are a number of starting thresholds that can be selected by the human (the user) for initial segmentation. Developing a general approach for a wide range of MRI datasets is another challenge with these techniques. A wide range of brain MRI resolutions and sequences has proven difficult to handle [104] automatically. Implementing these systems is difficult due to the problem-specific logical limitations, for instance, brain MRI information and intensity or the grey level that must be overcome.

3.1.2. Deformable Surface Model-Based

The energy functions are used to guide deformable surface model-based approaches in the development and modification of an automated dynamic curve (an active contour) in order for it to adapt to a neural surface. Models of the brain's surfaces are first defined and then "adapted" to the image of that brain in the image, using a tessellated mesh of triangles as an example. Constraints on the fitting generally fall into two categories.

The first segment's main goal is to keep the brain's surface well-conditioned and to match the brain's actual smoothness value. The second set of restrictions is to ensure that the model fits the brain surface perfectly. Deformation of the active contour model (also called curve evolution) is usually done iteratively until an adequate solution is found. Based on the picture intensity variation and the initial point of the fitting curve, these techniques are highly dependent. These characteristics can deceive researchers about the brain's proper boundaries and give either over or under segmented results.

A deformable model, fuzzy membership function, and image gradient detector were used by Suri [111] to segment the CerebroSpinal Fluid (CSF) and WM in MR images with an active contour. BET is the most popular and freely available algorithm in this field, developed by Smith, S.M. [104]. Brain MR images are analyzed using a "robust" lower- and upper-grey-scale value to determine the brain/non-brain threshold and the MRI's "centre of gravity". In order to fit the brain's surface, it employs a triangular tessellation of the surface of a sphere. This is also relatively quick, as it doesn't necessitate any kind of preprocessing or registration beforehand. BET couldn't extract the inferior brain slices' region if the brain MRI volume's centre of gravity were outside the head (slices with the neck) [9].

Model-based Level Set (MLS) approach was created by Zhuang et al. [122] to differentiate intracranial tissues from the skull around the brain MRI. Two factors determine curve growth in a level set equation (whose values describe the forces that influence the curve's speed of evolution). The mean curvature of the curve was used to determine the first term, and the intensity of the cortex in brain MRIs was used to determine the second term. The level set framework combined these two terms (forces) to develop the curve toward the brain surface. By employing an implicit deformable model, Liu et al. [67] developed a robust and automated method for extracting the brain's regions.

Radial Basis Functions (RBFs) from Wendland explain the model with low computing cost and a compact support property. 2D coronal and sagittal brain slices are used to identify the brain's

outlines. The results of these two views are combined to create a 3D volume of the brain. Wang et al. [116] recently proposed an article based on enhanced BET [104]. A dynamic mesh model of the brain's surface is developed to fit in MRIs. The brain mask was created using a polygon fill method. A ray-casting volume rendering technique is utilized to examine the brain's surface utilizing these produced masks once they have been built. These methods have the advantage of distinguishing between the external and internal boundaries of the brain simultaneously. Brain MRI skull stripping can be more precise and accurate when employing deformable surface model-based approaches rather than histogram thresholding or mathematical morphology. As a result of their poor performance in low-contrast and noisy MRI datasets, these methods are rarely employed.

3.1.3. Atlas or Library-Based Methods

The brain images are labelled using expert delineations of the brain MRIs in an atlas or library-based manner. The atlas, training, or library set is a subset of the tagged images. Expert knowledge can only be transferred if the target brain pictures are sufficiently similar to the training set. Prior to using these techniques, much pre-processing, such as intensity and spatial normalization, is generally required [49]. When there is no evident association between the intensity of skull pixel values in a brain MRI and brain areas, they can differentiate the brain from non-brain tissues. Brain segmentation was characterized as a preparatory stage in the cortical surface reconstruction process by Dale et al. [33] by incorporating an ellipsoidal template tessellated into the brain. It was created by Leung et al. [64] using a template library and non-linear atlas registration to generate a segmentation approach called Multiple-Atlas Propagation and Segmentation (MAPS). STPLE (Simultaneous Truth and Performance Level Estimation) is a method for creating and combining several segmentations from a manually segmented library's best-matched templates. The approach was developed and tested using ADNI subsets and manual measurements.

Brain MAPS, given by Leung et al. [63], compares template library-based brain segmentation to BET [104], BSE [101], and the Hybrid Watershed Algorithm (HWA) [96]. Eskildsen et al. [38] created BEaST, an automated brain extraction approach known as the non-segmentation framework and a multi-resolution framework. Patch-based segmentation is the technique's primary source of inspiration. [31], wherein the Sum of Squared Differences is used to calculate the distance between patches.

BEaST is significantly faster than previous label fusion algorithms and requires a far smaller prior library. Using information from the National Institutes of Health Pediatric Database, only 50 priors were created semi-automatically [112], the International Consortium for Brain Mapping (ICBM) [73], and the ADNI [79]. First, priors were normalized in terms of intensity and spatial resolution. We used a semi-automatic method to create brain masks for library priors' ground truth (or gold standard). BeaST-based label fusion is proposed by Manjon et al. [71] to improve accuracy while minimizing calculation time.

In order to achieve better standardization between the template library subjects, a new construction workflow for multi-atlas libraries has been established. The bilateral patch similarity measures, block-wise labelling methodology, and a regularization restriction have improved accuracy while saving cost. In [37], multi-atlas skull stripping was discussed. Based on multi-atlas registration, it addresses the issue of variability in imaging features between studies. After selecting a collection of templates, they used a study-specific template selection technique to best represent the anatomical variance within the dataset. To overcome the problems associated with the registration of brain images with the skull, an adaptive registration technique was proposed. This algorithm adaptively aligned distinct parts of the brain depending on the similarity and reliability of matching measurements. The co-registered template masks were finally joined using a spatially adaptive weighted

voting technique.

An automatic and adaptable algorithm for labelling 3D T1Wbrain MRIs in an adult was developed by Heckemann et al. [49]. Labels are transferred from several atlases using image registration and iterative refinement to a specific target brain picture. Every step of the algorithm provided a consensus label. As a result, the search for a border around this consensus label's boundary was limited. This algorithm (Pincram) can be downloaded for free from the [**?**] website.

Del Re et al. [34] used an innovative new (Multi-Atlas Brain Segmentation) MABS-based brain masking approach recently. By assigning weights to the atlases based on their similarity to the target image, MABS allows for greater flexibility and avoids the issue of atlas selection, unlike other atlas-based methods. More weight is given to atlases that closely resemble the target image than less similar atlases. Because both diseased and control photos are included in the training set, the MABS approach reduces the possibility of averaging individual differences. FreeSurfer (FS; version 5.3) [42], BET [104], and Brainwash [84] are also compared.

Accurate Learning with Few Atlases (ALFA) was developed by Ahmed Serag et al. [97] for multimodal newborn brain MRI brain extraction. When combined with a machine learning-based label fusion method that only requires a few atlases in low-dimensional data, the strategy gives a quick way to choose atlases. Furthermore, Roy and colleagues [91] have published a "spare patch-based multi-contrast brain stripping approach" (MONSTR) that creates a final mask using non-local patch information from several atlases. Additionally, this algorithm can be found online and is not affected by the disease. Among the most recent algorithms are [114]. The accuracy of Atlas or library-based approaches is impacted by the characteristics of spatial normalization, atlas registration, brain masks and intensity in each brain MRI volume. Furthermore, the computing effort required to apply these solutions is significant.

3.1.4. Region Growing and Watershed Method

In brain MRIs, Region Growth (RG) and watershed algorithms examine the pixels and merge neighboring picture pixels with uniformity features based on resemblance criteria to create different connected regions. At least one image pixel, called the seed, must be located in the region of interest in order for these approaches to work (ROI). Using a predefined similarity criterion, pixels in the vicinity of the seed are checked to see if they fall within the ROI (Region of Interest). The grayscale value of MRI pixels in the brain, as well as other characteristics of the imaging, can be utilized to assess and determine similarity criteria. The seed(s) can be chosen manually or automatically based on the attributes of the image. Repeated RG processes are carried out until the criterion for stopping has been met. Segmenting CT and MRI volumes in 3D using RG and morphological filters was devised by Hohne and his colleagues [50]. An SRG (3D Seeded Region Growing) approach for brain MRI segmentation has also been proposed by Justice and colleagues [60]. The 2D RG approach developed by Park and Lee [85] for brain T1-W MRIs was efficient and robust.

Histogram analysis was used to remove background voxels from the brain MRI volume in the first stage. A mask formed by morphological processes is then used to identify the brain and non-brain seed areas. A 2D RG method, based on generic brain structure knowledge, is used to enlarge the brain area from nearby pixels in the brain image. Only brain MRIs with a coronal orientation can benefit from this technique. Multispectral Adaptive Region Growing Algorithm (MARGA) was developed by Roura et al. [90] to overcome this barrier, allowing them to use their technique in axial views as well as low-quality brain images, and to offer a novel RG-based skull stripping technique. Complementary brain MRI data was used to acquire an initial seed region that was then extended using the 2D RGC. L. Wang et al. developed a level set technique for recovering the brain from MRI with contrast enhancement using a multistage formulation based on the energy required to fit

a certain Gaussian distribution [113]. Gaussian distributions with different mean and variances are used to model the image's intensity.

Methods based on region labelling, clustering, and 2D RG were proposed by Somasundaram et al. [107, 108], to remove the skull from the patient. Hahn et al. [47] presented a reliable and easy method for detecting brain tissues and deleting non-cerebral tissue using a modified 3D fast watershed transform in a T1-W. Segonne et al. [96] Using a deformable surface model, created a new hybrid HWA for brain segmentation [33] and the watershed technique [47]. According to Sadananthan et al. [94], the two algorithms [47] and [96] diverge in distinct places; hence, the presence of two algorithms would result in more robust conclusions for skull stripping. It is difficult to discriminate between distinct brain tissues on an MRI scan because of the Partial Volume Effect (PVE) [95], and the RG technique is restricted in its precision due to this problem. Additionally, the watershed algorithms tend to suffer from brain tissue over-segmentation.

3.1.5. Meta-Algorithms and Hybrid

A single algorithm may not extract the whole brain or remove the skull from all subjects in a brain MRI dataset. A wide range of techniques or manual involvement must be used to achieve satisfactory outcomes regarding the specifics. Many similar methods may be found in a single setting, making it easy to explore and test different techniques. Any algorithm's output can be interpreted. The best procedures can be selected automatically with an algorithmic meta-algorithm or hybrid approach that enables a general method to be required and produces a legitimate result no matter what input data is used in the algorithm. Image attributes, scanning protocol, such as image contrast, resolution, subject characteristics such as age and atrophy, as well as imaging signal to noise ratio, all influence skull stripping approaches for brain MRIs [41]. Each approach has its own merits and cons. It is also possible for algorithms to differ in their precision in many areas of the brain [54]. The contributions of each sub-algorithm should result in brain extraction results that are generally superior to any single method in a hybrid algorithm.

Brain MRI skull stripping can be improved with the help of hybrid methods that combine the advantages of two or more methodologies. Bauer et al. [13, 14] they used the Insight Segmentation and Registration Toolkit (ITK) to combine a level set-based methodology with a geodesic active contour brain segmentation method based on an atlas. "itk::StripTsImageFilter".

The brain has been successfully segmented in MRIs, CTs and FLAIR images with this hybrid approach. By attempting to run four different brain extractors, David E. Rex et al. [87] developed the Meta-Algorithm for brain extraction (along with BSE [101], BET [104], 3dIntracrnial [117], and Watershed from FreeSurfer [33]) in conjunction with a registration technique to intelligently integrate the findings of the brain extraction and obtain better outcomes than any of the separate algorithms.

In order to determine the best Boolean grouping of extraction procedures for a given voxel, the algorithm analyses training data voxel-by-voxel. Segonne et al. [96] created a new HWA for brain segmentation by combining a deformable surface model [33] and the watershed algorithm [47]. Although the deformable surface model efficiently combines the geometry information from the brain MRI, the intensity information from inside the brain cannot be retrieved. Watershed algorithms, on the other hand, do not take into account geometric information. It was found that their hybrid algorithm outperformed either strategy on its own. The approach of expectation maximization, mathematical morphology, connected component analysis, and active geodesic contours were used, Huang et al. [51] a new hybrid approach was introduced ROBEX, a well-known learning-based system, was presented by Iglesias et al. [55].

The graph section for whole-brain extraction integrates both a discriminative and generative model. An RF (Random Forest) classifier is used to identify the boundaries of the brain. To suit

the probabilistic output of RF, a point distribution model is utilized to constrain the growth of a triangular mesh. Using the graph segment section, the deformation (contour) is further tuned and optimized. Without any parameter adjustments, it performed better. The "ROBEX1.2" package of ROBEX is freely available at [83]. The ROBEX skull stripping approach was extended by William Speier et al. [109] to recover the brain from Glioblastoma Multiform (GBM) pictures. They used healthy brain MRIs to develop a form model that is generally impervious to lesions within the brain. Random Walker (RW) [46] corrects for leaking into the ventricles and uses adaptive thresholding to find probable resection voids at the brain boundary.

The "Simple Paradigm for Extra-Cerebral Tissue Removal (SPECTRE)" developed by Aaron et al. [20] is used for skull stripping. Elastic registration, brain tissue segmentation, and morphological methods based on the watershed concept are among the approaches used in this system. SPECTRE was built primarily for use in T1W brain MRIs. With a simple modification, the authors stated that it could be used with various imaging modalities (e.g., T2-W and PDW (Proton Density Weighted)). For paediatric brain MRIs, Shi et al. [103] presented a new meta-algorithm called "brain extraction and labelling (LABEL)." Skull stripping methods that have recently been developed include [45, 80]. When using meta-algorithms and hybrid approaches, it is necessary to train the data extensively to understand the specific brain properties needed to segment MRI scans of the brain appropriately.

3.2. CNN-Based or Deep Learning-Based

Different magnetic fields and viewpoint locations may be used for Brain MRIs. There is a lot of information in the image parameters, and it's relatively diversified. As a result, the development of algorithms requires a high degree of resilience to these changes. Skull-stripping approaches based on deep learning tend to be categorized into two separate groups: 2D and 3D methods. Although it is projected that 3D skull-stripping will produce higher outcomes, 2D skull-stripping has been more common than 3D procedures due to its computational cost. The two primary groups of 2D skull-stripping procedures may be summarized as follows. A voxel-wise neural network is in the first category, whereas a fully connected CNN is in the second. Multiple 2D CNNs are used to detect the voxel's centre and forecast its class in the first group of networks. The second category of networks has an encoder-decoder structure. While the encoder section extracts information from the image, the decoder extends the image to obtain high-resolution segmentation results. U-Net is one of the most widely used networks [89]. Because fully convolutional networks can recognize both local and global attributes, the algorithms of the second category are generally more efficient than those of the first. Fully convolutional networks are superior for image processing because they are faster and don't have the same constraints as the first group's methods.

3.2.1. 2D Skull-Stripping

The combination of the segmentations, the 2D semantic can predict the entire volume. When it comes to semantic segmentation, two-dimensional semantic segmentation is generally faster than three-dimensional semantic segmentation. A 2D slice is used as input; hence it does not consider the context of neighboring slices. 2D skull-stripping approaches based on neighboring information have been presented to address this issue, and some of them have shown comparable results to the 3D based methods with less processing. One method proposed by Salehi et al. [77] was a fully convolutional network. A parallel two-dimensional FCN U-Net and two parallel voxel-wise networks are demonstrated. Each network is followed by an auto-context CNN classifier. It was known as Auto-Net.

Because 3D CNNs are computationally expensive, the authors advocated employing two networks instead. In the first network, three 2D networks (axial, coronal, and sagittal) are employed instead of

a 3D CNN. From the input, the two-dimensional network receives the image in three different patch sizes. Three distinct patches are required to obtain both local and global information.

Compared to 3D CNN, this network contains significantly fewer parameters, but it performs just as well. According to [89], the second proposed network is all-convolutional. Auto-context algorithms combine low-level appearance features with high-level appearance features to provide contextual information. Auto-Net has no end-to-end form because it requires a trained model in each plane to use auto-context. As proposed in the paper Lucena et al. [70], there are two main pieces to the network.

In the first section, there are three 2D CNNs, and the second part is a context-aware network. Using three 2D CNNs, we can cover three spatial dimensions (axial, coronal, and sagittal), called CONSNet. By using a tri-planar technique, the authors were able to outperform the one-way procedure. Concatenation is used to create 3D segmentation from the output of 2D prediction. Instead of using gold-standard masks as the basis for their findings, the authors opted to employ "silver standard" masks. The term "silver standard masks" refers to the agreement-generated labels using publicly available non-deep learning-based skull-stripping procedures. Professionals handcraft the best gold standard masks.

According to the study, even though the CC-359 dataset was used to train the suggested technique, it outperformed the LPBA40 and the OASIS datasets. A considerable advantage of using silver standards is that it considerably minimizes the expense of manually annotating. Automated skull-stripping methods were combined to produce silver-standard masks. 2D FCN U-Net was also used by Lucena et al. [69]. The model was trained using standard silver masks, and the authors stated that it performed similarly to standard gold masks in terms of generalization. Silver standard masks can also be utilized to enhance the data and eliminate the requirement for manual segmentation; according to this study, Carmo et al. [21] used 2D FCN U-Net to partition the hippocampus in three planes. Instead of installing more networks, they have come up with a better solution. The activation heat map was added to each 2D FCN U-Net, and a specified threshold was applied before 3D labelling was performed. This technique outperformed Lucena et al. [69] by a wide margin.

Yilmaz et al. employed the Multistable Cellular Neural Network using MRI for Skull Stripping [118] to accomplish skull stripping (mCNN-MRI-SS). They suggested employing a linear image combining approach to boost contrast prior to preprocessing. This results in a reduction in noise and an increase in contrast. The Artificial Bee Colony (ABC) algorithm determines all training parameters. The ABC algorithm is a swarm intelligence-based optimization algorithm.

The ABC algorithm is recommended because it provides a large multidimensional search area for solving coefficient parameters, templates, and output functions, according to the authors. On superior and inferior slices, mCNN-MRI-SS performed similarly to or worse than BET and BSE, with identical or worse results. It's possible that this is due to errors in the analytical computations. The calculation time is slower than other algorithms since the analysis algorithm is applied to all particles.

It was hypothesized in the subsequent research that a Confidence Segmentation Convolutional Neural Network (CSCNet) might be used for skull stripping [28]. The encoder-decoder structure was chosen by CSCNet. SegNet is one of the most often used networks in semantic segmentation [10]. The sole variation between SegNet and the author is that the author employed the ReLU activation function instead of the softmax function. Using this ReLU function, an image's confidence level can be calculated. Confidence level matrices were used to build a bitmask that was applied to the original MR picture. Because the author's model is unable to generate accurate brain tissue, they rely on the activation function that has been trained on the target image. For example, the more active you are, the more dependable you are. Although CSCNet does not handle artefacts as well as the other

approaches, it is superior to them.

It was proposed by Duy et al. [81] to bring the benefits of the Active Shape Model (ASM) and CNN together. ASM [30] is a statistical model that changes data iteratively in order to find the target object in a new image. Face image analysis and medical imaging are two of the most common uses of ASM. Each feature point must have its attribute information checked for before moving on to the ASM process can begin. Highlights of this work include the following. Sagittal planes are used instead of 3D components in brain imaging since they are identical in all directions. Using data from the first half to forecast the second half allows for more accurate segmentation. According to the authors' criteria, the brain can be split into three categories. The most minor but most complicated group is the first; the most extensive but least complicated is the third group. Slices in each group are highly similar in shape. The algorithm can accomplish high-accuracy segmentation since it has a comparable form.

When it comes to determining where the bounds of the image are, ASM is employed. The second and third groups are the first to benefit from ASM implementation. Post-processing methods such as a CNN, a conditional random field, and a Gaussian process enhance the ASM contour. To make it easier for CNN to cope with the first group, segmentation findings are provided to the CNN that processes the second group. When the form of the test image matches the shape of the training image, ASM imitates a high-performance level.

In MRI scanned images, the skull and the brain appear nearly identical, making it difficult to tell them apart. Dey et al. [35] came up with the notion of a CompNet network to overcome this challenge. Encoder-decoder networks were used in the network. First, it teaches about the properties of brain tissue, and then it moves on to a complementary portion found somewhere else in the body.

The brain can be extracted from MRIs using this method. The authors devised a sub-encoder-decoder network in order to recreate the original encoder-decoder network depending on the results of both branches. Direct feedback is provided to networks that process brain sections and their complementary portions in order to recreate the original one. When compared to well-known networks like U-Net and dense U-Net, Optimal CompNet's accuracy is superior.

Brain segmentation methods such as FMRIB Software Library (FSL) [59], SPM (Statistical Parametric Mapping) [7], and others [62] can be mimicked using NeuroNet [86]. A 5000 automatically segmented T1-weighted brain MRI data were used to train the network. The network is laid out as follows. A single encoder and multiple decoders derive the final result from the encoder's output. The state-of-the-art brain segmentation tool is taught to each decoder. Overlapping label maps make it possible to generate several outcomes from the same model. It also saves time because it can cause multiple results at once.

Networks, according to the authors, are extremely resilient to changes in input data. Additionally, Neuronet does not necessitate any of the usual preprocessing steps. There are no additional hyper-parameters necessary for the network to provide output from raw photos. The subsequent introduction of deep learning algorithms that are extensively utilized for general 2D semantic segmentation and applied to the skull-stripping problem will be introduced. There was a significant improvement in semantic segmentation using FCN (Fully Convolutional Networks) [102]. A substantial difference between FCN and prior semantic segmentation articles is that it removes the fully connected layer. Because of the fully connected layer, existing papers had difficulty with location information being eliminated. Because of this, the authors of FCN decided to replace the fully linked layer with a 1×1 convolution layer. The image was then upsampled to recreate its original dimensions. As a result of combining the encoder's output after interpolation, segmentation results are obtained in more fine-grained detail. 2015 saw the release of SegNet [10].

In the same way, as FCN uses encoder-decoder designs, this network does the same. Maxpooling's

indices are shifted to maximize memory efficiency instead of replicating encoder functionality, and shortcut connections are used more frequently. Another network layout that resembles the earlier FCN and SegNet is U-Net [89]. This network is split into two sections: one that is contracting and the other that is growing. The global context and local details are determined using both the contracting and expanding routes. By concatenating the output of the contracting approach before each up convolution, U-Net enables for more precise localisation. DeepLab uses atrous convolution to address the semantic segmentation problem. Semantic segmentation was initially being performed using atrous convolution in DeepLab V1 [24]. Atrous convolution is a new method for convolution filtering that makes the stride between the elements. The filter can cover a larger area with a similar amount of variables as the distance increases. The size of the receptive field heavily influences semantic segmentation performance, so having a large receptive field without adding computation is highly advantageous.

Atrous Spatial Pyramid Pooling (ASPP) was proposed by DeepLab V2 [25] to apply several contexts. The method concatenates the results of atrous convolutions performed over varied distances. It is feasible to reliably identify multiscale contexts by recognizing all local and global aspects using this method. DeepLab V3 uses an atrous convolution in existing ResNet topologies [27] provided a more dense feature map. Convolution that combines separable and atrous convolution was proposed by DeepLab V3+ [26]. A decoder comparable to U-Net was used to replace the decoder that was simply upsampled bilinearly. Because of this, separable convolution was used to boost encoder, ASPP, and decoder performance.

It was published in Arxiv at the end of 2016, the RefineNet [66], which was suggested using current encoder and decoder networks instead of dilated/atrous convolutions. Upsampling low-resolution features before entering the encoded result into the decoder is done in RefineNet. This enables the collection of contextual data. Deep learning techniques can be compared on the voc2012 [39] dataset for their average precision.

3.2.2. 3D Skull-Stripping

Is unlike the 2D method, can take advantage of all three-dimensional information, resulting in improved outcomes in segmentation. In addition to that, it requires an enormous amount of calculation. One convolutional softmax output layer and seven hidden 3D convolutional hidden layers have been proposed. by Kleesiek et al. [61], wherein this network was built exclusively for skull stripping.

Thus, the scientists sought to encompass the range of ages, shapes and sizes of brains with slight parameter adjustment. As a further objective, the network was designed to support any single modality or a mix of many modalisms (T1-W, T2-W, T2-FLAIR, etc.). The author experimented with several different architectures by varying the number of layers and concluded that the one proposed has the best performance. On the OASIS [72], LPBA40 [100] and IBSR [88] datasets, Kleesiek's [61] technique outperformed the most widely used conventional methods (BET, BSE, Robex, etc.) in terms of dice and specificity, but only averagely surpassed them in terms of sensitivity. Using the universal 3D segmentation network, 3D-UNet, for skull-stripping difficulties was suggested by Hwang et al. [54]. The authors demonstrated that the method's performance is comparable to that of Kleesiek et al [61]. On the NFBS dataset, Kleesiek and colleagues' network performed better in dice and specificity, whereas 3D-UNet performed better in sensitivity tests. An improved performance was demonstrated by Huo and colleagues [53], employing both the traditional and deep learning methods combined. The network's capabilities are limited since it learns spatial and contextual information from a large number of image patches, and the amount of medical images available for training is insufficient. The author presented Spatially Localized Atlas Network Tiles

(SLANT) to address these two issues. The spatial limitation was overcome by employing many networks spread across a wide area. Each network was honed using a set of pre-installed fixes. A multi-network approach allows each network to focus on detecting the differences between patches that are quite similar. Affinity registration and intensity normalization were employed in advance to make this method possible.

Label fusion was then utilized to create the final product from the network tiles themselves. The authors created auxiliary labels from 5111 unlabeled scans in order to expand the number of training image sets. The multi-atlas segmentation was used to create the auxiliary labels. The method's major drawback is the enormous amount of computing power it necessitates. Increasing the number of network tiles has a linear effect on training and testing times on a single GPU. U-Net was the foundation for the Isensee et al. [57] network, which they then enhanced. The authors' goal was to develop a network that could withstand changes in brain tissue caused by disease or treatment while also remaining unaffected by changes in MRI hardware. This is how they've changed it. The encoder section of U-Net was first populated with pre-activation residual blocks, and the block results were merged with the original one. Gradient flow is boosted due to more profound network architecture. The dimensions of $128 \times 128 \times 128$ voxels and $1.5 \times 1.5 \times 1.5 mm^3$ are representing patch size and voxel resolution, respectively. However, a full-sized patch size enables a precise reconstruction of the brain mask, no matter which parts are lost in an accident. An additional loss layer was built. It is quite challenging to train the deepest regions of U-Net because of chain rules. Thus, the authors attempted to address this issue by including additional loss layers in the deep part of their algorithm. Lastly, the activation and normalization functions were altered. The leakyReLU process replaced the ReLU function, which was determined to collapse in deep networks. The batch size is less in the suggested method than in other methods.

Consequently, there is a lack of stability in the batch means and standard deviation; as a result, instead of using batch normalizing, the authors used instance normalization. Essentially, each batch normalizes on its own, without regard to the previous batches. HD-BET is projected to operate in a broad spectrum of neuroradiological illnesses, even though Isensee's approach was only applied to tumours and normal brains.

The volumetric dilated convolutions were first proposed by Fedorov et al. [40] as a foundation for a deep learning model. Atrous convolutions, as introduced by DeepLab [24], are also known as dilated convolutions. This model has fewer parameters than other models, which reduces processing time and increases test data correctness. Furthermore, this model was able to perform well even if it was trained on faulty data. Three new methods are provided by FRnet [121], the U-Net was used as a starting point by the authors. When FRnet and U-Net decode, the residual block is executed after a "de-convolution + batch normalization + ReLU" block in the decoder section. Convolution being used before concatenation is also a first. In addition, A new loss function was used to emphasize unclear or vague boundary regions. Because the boundary is always an essential section of the segmentation map, the loss function is weighted at the boundary area.

There is also a deep learning framework for dealing with neuroimaging that was developed by Beers and colleagues [15]. On the other hand, while several packages excel in sharing and designing deep learning algorithm implementations, only a few include tools for working with clinical data. The authors illustrated how a framework develops and trains a network using their toolkit, as well as how the present state-of-the-art architecture can be easily and quickly updated using their toolkit. In addition, the framework has shown consistent performance in a variety of contexts by offering pretreatment and post-processing often utilized in medical imaging. Users who lack coding skills are expected to benefit from the author's efforts to create a GUI interface.

The following section briefly describes deep learning-based solutions for 3D semantic segmentation

that have recently been proposed and are applied to the 3D skull-stripping problem. 3D U-Net [32] is the first of the networks to be discussed. The 2D U-Net model was used to develop this network, which was then extended by one dimension. Methods from 2D U-Net were adapted to 3D, but new one's such as batch normalization was also implemented [56]. Due to its ability to learn from poorly annotated volumetric pictures, this network has a lot of potentials. V-Net [75] similar to the 3D U-Net, this network has end-to-end structures. The basic components are an encoder and a decoder.

In contrast to previous networks, V-Net uses convolution layers and strides to down- and up-sample instead of pooling. The VoxRes module is one of 25 layers in VoxResNet [23]. The VoxRes module is a three-dimensional representation of ResNet's [48] remnant unit in three dimensions. In this case, every fourth block is deconvolved so that the final output can be classified and combined. This strategy has the advantage of incorporating information from multiple sources and mediums. An improved segmentation performance will occur since more information can be learned and various scales can be applied. There has been a call for DenseVoxNet [119]. Even with fewer parameters, this network is superior to 3D U-Net and VoxResNet. As with the VoxResNet, a DenseBlock is used to extend the DenseNet's three-dimensional connections [52]. A minor gradient vanishing problem and fewer learning parameters are among the advantages of DenseBlock. But despite their ability to automatically learn the most challenging feature representation representations from data, systems based on deep learning have limitations. When it comes to deep learning, it's difficult to explain how to acquire the outcome. A deep learning model is essentially a set of opaque containers. Deep learning is difficult to grasp and even more difficult to develop because of its obscurity. Because of this, deep learning model developers cannot change the model's various hyperparameters and increase its performance. It's not uncommon for them to be forced to rely only on ineffective methods like trial and error. Another issue is the restriction imposed by the reliance on specific data. A deep learning network model to be adequately trained requires a large amount of training data. Using deep learning algorithms is known to accomplish this. It has been done by creating multiple open databases for general photos, which continue to grow. To complicate matters, collecting large amounts of labelled datasets in medical photographs is typically complex, costly, and fraught with ethical and privacy considerations. The only way to deal with this data problem is to work together with other countries worldwide.

4. Conclusion

A suitable segmentation method for MR images is necessary for accurate diagnosis of brain patients in order to carry out enhanced diagnosis and therapy. There are currently several images from various slices that can be used for accurate diagnosis, planning, and therapy purposes. In order to make an informed decision, it is necessary to process a large amount of data.

Researchers no longer have to worry about computational speed. Because of this, the focus is on improving the information gained by slice orientation and completing segmentation in order to create an accurate picture of the brain, Consequently.

We've tried to summarise some of the best recent studies on skull stripping in this document. Using the literature, we discovered that the skull-stripping of brain MR images has been one of the most active study fields in recent years. Yet, no clinically acceptable automated approach exists at the moment.

References

[1] S. Ahmed, K.Y. Choi, J.J. Lee, B.C. Kim, G.-R. Kwon, K.H. Lee and H.Y. Jung, *Ensembles of patch-based classifiers for diagnosis of alzheimer diseases*, IEEE Access 7 (2019) 73373–73383.

[2] S.A. Al-Majeed and M.S.H. Al-Tamimi, *Survey based study: Classification of patients with alzheimer's disease*, Iraqi J. Sci. 61(11) (2020) 3104–3126.

[3] M.S.H. Al-Tamimi, A.S.H. Al-Tamimi and G. Sulong, *A new abnormality detection approach for T1-weighted magnetic resonance imaging brain slices using three planes*, Adv. Comput. 6(1) (2016) 6–27.

[4] M.S.H. Al-Tamimi and G. Sulong, *A review of snake models in medical MR image segmentation*, J. Teknol. (Sci. Eng.) 69(2) (2014) 101–106.

[5] M.S.H. Al-Tamimi and G. Sulong, *A new method for detecting cerebral tissues abnormality in magnetic resonance images*, Mod. Appl. Sci. 9(8) (2015) 363–379.

[6] M.S.H. Al-Tamimi, G. Sulong and I.L. Shuaib, *Alpha shape theory for 3D visualization and volumetric measurement of brain tumor progression using magnetic resonance images*, Magn. Reson. Imag. 33(6) (2015) 787–803.

[7] J. Ashburner and K.J. Friston, *Voxel-based morphometry - the methods*, Neuroimage 11(6I) (2000) 805–821.

[8] M.S. Atkins and B.T. Mackiewich, *Fully automatic segmentation of the brain in MRI*, IEEE Trans. Med. Imag. 17(1) (1998) 98–107.

[9] M.S. Atkins, K. Siu, B. Law, J.J. Orchard and W.L. Rosenbaum, *Difficulties of T1 brain MRI segmentation techniques*, Med. Imag. 2002 Image Process 4684(2002) (2002) 1837.

[10] V. Badrinarayanan, A. Kendall and R. Cipolla, *SegNet: A deep convolutional encoder-decoder architecture for image segmentation*, IEEE Trans. Pattern Anal. Mach. Intell. 39(12) (2017) 2481–2495.

[11] A.G.R. Balan, A.J.M. Traina, M.X. Ribeiro, P.M.A. Marques and C. Traina, *Smart histogram analysis applied to the skull-stripping problem in T1-weighted MRI*, Comput. Biol. Med. 42(5) (2012) 509–522.

[12] S. Bao and A.C.S. Chung, *Multi-scale structured CNN with label consistency for brain MR image segmentation*, Comput. Methods Biomech. Biomed. Eng. Imaging Vis. 6(1) (2018) 113–117.

[13] S. Bauer, T. Fejes and M. Reyes, *A skull-stripping filter for ITK*, Insight J. (2012) 1–7.

[14] S. Bauer, L.-P. Nolte and M. Reyes, *Skull-stripping for tumor-bearing brain images*, Annual Meeting of the Swiss Society for Biomedical Engineering, 2012.

[15] A. Beers, J. Brown, K. Chang, K. Hoebel, J. Patel, K.I. Ly, S.M. Tolaney, P. Brastianos, B. Rosen, E.R. Gerstner and J. Kalpathy-Cramer, *Deepneuro: An open-source deep learning toolbox for neuroimaging*, Neuroinformatics 19(1) (2021) 127–140.

[16] C.C. Benson and V.L. Lajish, *Morphology based enhancement and skull stripping of MRI brain images*, Proc. 2014 Int. Conf. Intell. Comput. Appl. ICICA 2014 (2014) 254–257.

[17] J. Bernal, K. Kushibar, M. Cabezas, S. Valverde, A. Oliver and X. Llado, *Quantitative analysis of patch-based fully convolutional neural networks for tissue segmentation on brain magnetic resonance imaging*, IEEE Access 7 (2019) 89986–90002.

[18] A.S. Bhadauria, V. Bhateja, M. Nigam and A. Arya, *Skull stripping of brain MRI using mathematical morphology*, Proc. Second Int. Conf. SCI 1 (2018) 775–780.

[19] M.E. Brummer, R.M. Mersereau, R.L. Eisner and R.R.J. Lewine, *Automatic detection of brain contours in MRI data sets*, Lect. Notes Comput. Sci. 511(2) (1991) 189–204.

[20] A. Carass, J. Cuzzocreo, M.B. Wheeler, P.L. Bazin, S.M. Resnick and J.L. Prince, *Simple paradigm for extra-cerebral tissue removal: Algorithm and analysis*, Neuroimage 56(4) (2011) 1982–1992.

[21] D. Carmo, B. Silva, C. Yasuda, L. Rittner and R. Lotufo, *Extended 2D consensus hippocampus segmentation*, arXiv preprint arXiv:1902.04487, (2019).

[22] C.C. Chen, H.-C. Chen, H.C. Wang, Y.-C. Chang, Y.-Y. Wu, W.-H. Chen, H.-M. Chen, S.-K. Lee and C.-I. Chang, *An iterative mixed pixel classification for brain tissues and white matter hyperintensity in magnetic resonance imaging*, IEEE Access 7 (2019) 124674–124687.

[23] H. Chen, Q. Dou, L. Yu, J. Qin and P.A. Heng, *Voxresnet: Deep voxelwise residual networks for brain segmentation from 3D MR images*, Neuroimage 170 (2018) 446–455.

[24] L.C. Chen, G. Papandreou, I. Kokkinos, K. Murphy and A.L. Yuille, *Semantic image segmentation with deep convolutional nets and fully connected CRFs*, IEEE Trans. Pattern Anal. Mach. Intell. 40(4) (2015).

[25] L.C. Chen, G. Papandreou, I. Kokkinos, K. Murphy and A.L. Yuille, *Deeplab: semantic image segmentation with deep convolutional nets, atrous convolution, and fully connected CRFs*, IEEE Trans. Pattern Anal. Mach. Intell. 40(4) (2017) 834–848.

[26] L.-C. Chen, G. Papandreou, F. Schroff and H. Adam, *Encoder-decoder with atrous separable convolution for semantic image segmentation*, Pertanika J. Trop. Agric. Sci. 34(1) (2011) 137–143.

[27] L.-C. Chen, G. Papandreou, F. Schroff and H. Adam, *Rethinking atrous convolution for semantic image segmentation*, arXiv preprint arXiv:1706.05587, (2017).

[28] K. Chen, J.-S. Shen, F. Scalzo, *Skull stripping using confidence segmentation convolution neural network*, International Symposium on Visual Computing, Springer, Cham. (2018) 15–24.

[29] J. Chiverton, K. Wells, E. Lewis, C. Chen, B. Podda and D. Johnson, *Statistical morphological skull stripping of adult and infant MRI data*, Comput. Biol. Med. 37(3) (2007) 342–357.

[30] T.F. Cootes, C.J. Taylor, D.H. Cooper and J. Graham, *Active shape models–their training and application*, Computer Vision and Image Understand. 61(1) (1995) 38–59.

[31] P. Coupé, J.V. Manjón, V. Fonov, J. Pruessner, M. Robles and D.L. Collins, *Patch-based segmentation using expert priors: Application to hippocampus and ventricle segmentation*, Neuroimage 54(2) (2011) 940–954.

[32] Ö. Çiçek, A. Abdulkadir, S.S. Lienkamp, T. Brox and O. Ronneberger, *3D U-net: learning dense volumetric segmentation from sparse annotation*, Proc. Int. Conf. Med. Image Comput. Computer-Assisted Intervention, Athens, Greece, (2016) 424–432.

[33] M.I. Dale, A.M. Fischl, B. Sereno, *Cortical surface-based analysis: I. segmentation and surface reconstruction*, Neuroimage 9(2) (1999) 195–207.

[34] E.C. Del Re, Y. Gao, R. Eckbo, T.L. Petryshen, G.A.M. Blokland, L.J. Seidman, J. Konishi, J.M. Goldstein, R.W. McCarley, M.E. Shenton and S. Bouix, *A new MRI masking technique based on multi-atlas brain segmentation in controls and schizophrenia: A rapid and viable alternative to manual masking*, J. Neuroimag. 26(1) (2016) 28–36.

[35] R. Dey and Y. Hong, *Compnet: Complementary segmentation network for brain MRI extraction*, Lect. Notes Comput. Sci. 11072 (2018) 628–636.

[36] J. Dolz, C. Desrosiers and I. Ben Ayed, *3D fully convolutional networks for subcortical segmentation in MRI: A large-scale study*, Neuroimage 170 (2018) 456–470.

[37] J. Doshi, G. Erus, Y. Ou, B. Gaonkar and C. Davatzikos, *Multi-atlas skull-stripping*, Acad. Radiol. 20(12) (2013) 1566–1576.

[38] S.F. Eskildsen, P. Coupé, V. Fonov, J.V. Manjón, K.K. Leung, N. Guizard, S.N. Wassef, L.R. Østergaard, D.L. Collins and Alzheimer's Disease Neuroimaging Initiative, *Beast: Brain extraction based on nonlocal segmentation technique*, Neuroimage 59(3) (2012) 2362–2373.

[39] M. Everingham, L. Van-Gool, C.K.I. Williams, J. Winn and A. Zisserman, *The PASCAL visual object classes challenge 2012 (VOC2012) results*, http://www.pascal-network.org/challenges/VOC/voc2012/workshop/index.html, (2012).

[40] A. Fedorov, J. Johnson, E. Damaraju, A. Ozerin, V. Calhoun and S. Plis, *End-to-end learning of brain tissue segmentation from imperfect labeling*, Proc. Int. Jt. Conf. Neural Networks 2017 (2017) 3785–3792.

[41] C. Fennema-Notestine, I.B. Ozyurt, C.P. Clark, S. Morris, A. Bischoff-Grethe, M.W. Bondi, T.L. Jernigan, B. Fischl, F. Segonne, D.W. Shattuck, R.M. Leahy, D.E. Rex, A.W. Toga, K.H. Zou and G.G. Brown, *Quantitative evaluation of automated skull-stripping methods applied to contemporary and legacy images: Effects of diagnosis, bias correction, and slice location*, Hum. Brain Mapp. 27(2) (2006) 99–113.

[42] B. Fischl, *FreeSurfer*, Neuroimage 62(2) (2012) 774–781.

[43] F.J. Galdames, F. Jaillet and C.A. Perez, *An accurate skull stripping method based on simplex meshes and histogram analysis for magnetic resonance images*, J. Neurosci. Methods, 206(2) (2012) 103–119.

[44] O. Gambino, E. Daidone, M. Sciortino, R. Pirrone and E. Ardizzone, *Automatic skull stripping in MRI based on morphological filters and fuzzy C-means segmentation*, Proc. Annu. Int. Conf. IEEE Eng. Med. Biol. Soc. EMBS (2011) 5040–5043.

[45] Y. Gao, J. Li, H. Xu, M. Wang, C. Liu, Y. Cheng, M. Li, J. Yang and X. Li, *A multi-view pyramid network for skull stripping on neonatal T1-weighted MRI*, Magn. Reson. Imag. 63 (2019) 70–79.

[46] L. Grady, *Random walks for image segmentation*, IEEE Trans. Pattern Anal. Mach. Intell. 28(11) (2006) 1768–1783.

[47] H.K. Hahn and H.O. Peitgen, *The skull stripping problem in MRI solved by a single 3D watershed transform*, Lect. Notes Comput. Sci. 1935 (2000) 134–143.

[48] K. He, X. Zhang, S. Ren and J. Sun, *Deep residual learning for image recognition*, Proc. IEEE Computer Soc. Conf. Comput. Vision Pattern Recogn. 2016 (2016) 770–778.

[49] R.A. Heckemann, C. Ledig, K.R. Gray, P. Aljabar, D. Rueckert, J.V. Hajnal and A. Hammers, *Brain extraction using label propagation and group agreement: Pincram*, PLoS One 10(7) (2015) 1–18.

[50] W.A. Hohne, K.H. Hanson, Interactive 3D segmentation of MRI and CT volumes using morphological operations, J. Comput. Assist. Tomogr., 16(2) (1992) 285-294.

[51] A. Huang, R. Abugharbieh, R. Tam and A. Traboulsee, *MRI brain extraction with combined expectation maximization and geodesic active contours*, Sixth IEEE Int. Symp. Signal Process. Inf. Technol. ISSPIT, 107(1) (2006) 107–111.

[52] G. Huang, Z. Liu, L. Van Der Maaten, and K.Q. Weinberger, *Densely connected convolutional networks*, Proc. 30th IEEE Conf. Comput. Vis. Pattern Recognition, CVPR 2017 (2017) 2261–2269.

[53] Y. Huo, Z. Xu, Y. Xiong, K. Aboud, P. Parvathaneni, S. Bao, C. Bermudez, S.M. Resnick, L.E. Cutting and

B.A. Landman, *3D whole brain segmentation using spatially localized atlas network tiles*, Neuroimage 194 (2019) 105–119.

[54] H. Hwang, H.Z.U. Rehman and S. Lee, *3D U-net for skull stripping in brain MRI*, Appl. Sci. 9(3) (2019) 1–15.

[55] J.E. Iglesias, C.Y. Liu, P.M. Thompson and Z. Tu, *Robust brain extraction across datasets and comparison with publicly available methods*, IEEE Trans. Med. Imag. 30(9) (2011)1617–1634.

[56] S. Ioffe and C. Szegedy, *Batch normalization: Accelerating deep network training by reducing internal covariate shift sergey*, 32nd Int. Conf. Mach. Learn. ICML 2015(1) (2015) 448–456.

[57] F. Isensee, M. Schell, I. Pflueger, G. Brugnara, D. Bonekamp, U. Neuberger, A. Wick, H.-P. Schlemmer, S. Heiland, W. Wick, M. Bendszus, K.H. Maier-Hein and P. Kickingereder, *Automated brain extraction of multi-sequence MRI using artificial neural networks*, Hum. Brain Mapp. 40(17) (2019) 4952–4964.

[58] C.R. Jack, M.A. Bernstein, N.C. Fox, P. Thompson, G. Alexander, D. Harvey, B. Borowski, P.J. Britson, J.L. Whitwell, C. Ward, A.M. Dale, J.P. Felmlee, J.L. Gunter, D.L.G. Hill, R. Killiany, N. Schuff, S. Fox-Bosetti, C. Lin, C. Studholme, C.S. DeCarli, G. Krueger, H.A. Ward, G.J. Metzger, K.T. Scott, R. Mallozzi, D. Blezek, J. Levy, J.P. Debbins, A.S. Fleisher, M. Albert, R. Green, G. Bartzokis, G. Glover, J. Mugler and M.W. Weiner, *The alzheimer's disease neuroimaging initiative (ADNI): MRI methods*, J. Magn. Reson. Imag. 27(4) (2008) 685–691.

[59] M. Jenkinson, C.F. Beckmann, T.E.J. Behrens, M.W. Woolrich and S.M. Smith, *FSL*, Neuroimage 62(2) (2012) 782–90.

[60] R.K. Justice, E.M. Stokelyt, J.S. Strobel, R.E. Ideker and W.M. Smith, *Medical image segmentation using 3-D seeded region growing*, Med. Imaging 1997 Image Process 3034(205) (1997) 900–910.

[61] J. Kleesiek, G. Urban, A. Hubert, D. Schwarz, K. Maier-Hein, M. Bendszus and A. Biller, *Deep MRI brain extraction: A 3D convolutional neural network for skull stripping*, Neuroimage 129 (2016) 460–469.

[62] C. Ledig, R.A. Heckemann, A. Hammers, J.C. Lopez, V.F.J. Newcombe, A. Makropoulos, J. Lötjönen, D.K. Menon and D. Rueckert, *Robust whole-brain segmentation: Application to traumatic brain injury*, Med. Image Anal. 21(1) (2015) 40–58.

[63] K.K. Leung, J. Barnes, M. Modat, G.R. Ridgway, J.W. Bartlett, N.C. Fox, S. Ourselin and Alzheimer's Disease Neuroimaging Initiative, *Brain MAPS: An automated, accurate and robust brain extraction technique using a template library*, Neuroimage 55(3) (2011) 1091–1108.

[64] K.K. Leung, J. Barnes, G.R. Ridgway, J.W. Bartlett, M.J. Clarkson, K. Macdonald, N. Schuff, N.C. Fox, S. Ourselin and Alzheimer's Disease Neuroimaging Initiative, *Automated cross-sectional and longitudinal hippocampal volume measurement in mild cognitive impairment and alzheimer's disease*, Neuroimage 51(4) (2010) 1345–1359.

[65] P. Li, Y. Zhao, Y. Liu, Q. Chen, F. Liu and C. Gao, *Temporally consistent segmentation of brain tissue from longitudinal MR data*, IEEE Access 8 (2020) 3285–3293.

[66] G. Lin, A. Milan, C. Shen and I. Reid, *RefineNet: Multi-path refinement networks for high-resolution semantic segmentation*, Cvpr (2017) 1925–1934.

[67] J.X. Liu, Y.S. Chen and L.F. Chen, *Accurate and robust extraction of brain regions using a deformable model based on radial basis functions*, J. Neurosci. Methods, 183(2) (2009) 255–266.

[68] M. Liu, J. Zhang, E. Adeli and D. Shen, *Landmark-based deep multi-instance learning for brain disease diagnosis*, Med. Image Anal. 43 (2018) 157–168.

[69] O. Lucena, R. Souza, L. Rittner, R. Frayne and R. Lotufo, *Silver standard masks for data augmentation applied to deep-learning-based skull-stripping*, Proc. Int. Symp. Biomed. Imag. 2018 (2018) 1114–1117.

[70] O. Lucena, R. Souza, L. Rittner, R. Frayne and R. Lotufo, *Convolutional neural networks for skull-stripping in brain MR imaging using silver standard masks*, Artif. Intell. Med. 98 (2019) 48–58.

[71] J.V. Manjón, S.F. Eskildsen, P. Coupé, J.E. Romero, D.L. Collins and M. Robles, *Nonlocal intracranial cavity extraction*, Int. J. Biomed. Imag. (2014) 1–11.

[72] D.S. Marcus, A.F. Fotenos, J.G. Csernansky, J.C. Morris and R.L. Buckner, *Open access series of imaging studies (OASIS): Cross-sectional MRI data in young, middle aged, nondemented, and demented older adults*, J. Cogn. Neurosci. 22(12) (2010) 2677–2684.

[73] J.C. Mazziotta, A.W. Toga, A. Evans, P. Fox and J. Lancaster, *A probabilistic atlas of the human brain: theory and rationale for its development*, NeuroImage 2(2) (1995) 89–101.

[74] R. Mehta, A. Majumdar and J. Sivaswamy, *Brainsegnet: A convolutional neural network architecture for automated segmentation of human brain structures*, J. Med. Imag. 4(2) (2017) 024003.

[75] F. Milletari, N. Navab and S.A. Ahmadi, *V-Net: Fully convolutional neural networks for volumetric medical image segmentation*, Proc. 4th Int. Conf. 3D Vision, 3DV 2016, (2016) 565–571.

[76] P. Moeskops, M.J.N.L. Benders, S.M. Chiţ, K.J. Kersbergen, F. Groenendaal, L.S. de Vries, M.A. Viergever and I. Išgum, *Automatic segmentation of MR brain images of preterm infants using supervised classification*,

Neuroimage 118 (2015) 628–641.

[77] S.S. Mohseni Salehi, D. Erdogmus and A. Gholipour, *Auto-context convolutional neural network (auto-net) for brain extraction in magnetic resonance imaging*, IEEE Trans. Med. Imag. 36(11) (2017) 2319–2330.

[78] J.C. Morris, *The clinical dementia rating (CDR): Current version and scoring rules*, Neurology 43(11) (1993) 2412–2414.

[79] S.G. Mueller, M.W. Weiner, L.J. Thal, R.C. Petersen, C. Jack, W. Jagust, J.Q. Trojanowski, A.W. Toga and L. Beckett, *The alzheimer's disease neuroimaging initiative*, Neuroimaging Clin. N. Am. 15(4) (2005) 869–877.

[80] N.E.L. Narváez and E.E.Z. Varela, *A new approach on skull stripping of brain MRI based on saliency detection using dictionary learning and sparse coding*, Prospectiva 17(2) (2019).

[81] D.H.M. Nguyen, D.M. Nguyen, M.T.N. Truong, T. Nguyen, K.T. Tran, N.A. Triet, P.T. Bao and B.T. Nguyen, *ASMCNN: An efficient brain extraction using active shape model and convolutional neural networks*, Inf. Sci. 591 (2022) 25–48.

[82] D. Nie, L. Wang, Y. Gao and D. Sken, *Fully convolutional networks for multi-modality isointense infant brain image segmentation*, Proc. Int. Symp. Biomed. Imag. 2016 (2016) 1342–1345.

[83] NITRC, *Robust brain extraction (ROBEX)*, J.E. ROBEX 1.2., https://www.nitrc.org/projects/robex, (2013).

[84] NITRC, *Automatic registration toolbox (ART)*, http://www.nitrc.org/projects/art, (2020).

[85] J.G. Park and C. Lee, *Skull stripping based on region growing for magnetic resonance brain images*, Neuroimage, 47(4) (2009) 1394–1407.

[86] M. Rajchl, N. Pawlowski, D. Rueckert, P.M. Matthews and B. Glocker, *NeuroNet: Fast and robust reproduction of multiple brain image segmentation pipelines*, arXiv preprint arXiv:1806.04224, (2018) 1–9.

[87] D.E. Rex, D.W. Shattuck, R.P. Woods, K.L. Narr, E. Luders, K. Rehm, S.E. Stoltzner, D.A. Rottenberg and A.W. Toga, *A meta-algorithm for brain extraction in MRI*, Neuroimage 23(2) (2004) 625–637.

[88] T. Rohlfing, *Image similarity and tissue overlaps as surrogates for image registration accuracy: Widely used but unreliable*, IEEE Trans. Med. Imag. 31(2) (2012) 153–163.

[89] O. Ronneberger, P. Fischer and T. Brox, *U-net: Convolutional networks for biomedical image segmentation*, Int. Conf. Med. Image Comput. Computer-Assisted Interven. (2015) 234–241.

[90] E. Roura, A. Oliver, M. Cabezas, J.C. Vilanova, A. Rovira, L. Ramió-Torrentà and X. Lladó, *MARGA: Multispectral adaptive region growing algorithm for brain extraction on axial MRI*, Comput. Methods Programs Biomed. 113(2) (2014) 655–673.

[91] S. Roy, J.A. Butman and D.L. Pham, *Robust skull stripping using multiple MR image contrasts insensitive to pathology*, Neuroimage 146 (2017) 132–147.

[92] S. Roy and P. Maji, *An accurate and robust skull stripping method for 3-D magnetic resonance brain images*, Magn. Reson. Imaging, 54 (2018) 46–57.

[93] E.H. Rubin, M. Storandt, J.P. Miller, D.A. Kinscherf, E.A. Grant, J.C. Morris and L. Berg, *A prospective study of cognitive function and onset of dementia in cognitively healthy elders*, Arch. Neurol., 55(3) (1998) 395–401.

[94] S.A. Sadananthan, W. Zheng, M.W.L. Chee and V. Zagorodnov, *Skull stripping using graph cuts*, Neuroimage, 49(1) (2010) 225–239.

[95] M. Sato, S. Lakare, M. Wan and A. Kaufman, *A gradient magnitude based region growing algorithm for accurate segmentation*, in Proceedings 2000 International Conference on Image Processing (Cat. No. 00CH37101), (2000) 448–451.

[96] F. Ségonne, A.M. Dale, E. Busa, M. Glessner, D. Salat, H.K. Hahn and B. Fischl, *A hybrid approach to the skull stripping problem in MRI*, Neuroimage 22(3) (2004) 1060–1075.

[97] A. Serag, M. Blesa, E.J. Moore, R. Pataky, S.A. Sparrow, A.G. Wilkinson, G. Macnaught, S.I. Semple and J.P. Boardman, *Accurate learning with few atlases (ALFA): An algorithm for MRI neonatal brain extraction and comparison with 11 publicly available methods*, Sci. Rep. 6 (2016) 23470.

[98] Z.Y. Shan, G.H. Yue and J.Z. Liu, *Automated histogram-based brain segmentation in T1-weighted three-dimensional magnetic resonance head images*, Neuroimage 17(3) (2002) 1587–1598.

[99] D.W. Shattuck and R.M. Leahy, *Brainsuite: An automated cortical surface identification tool*, Lect. Notes Comput. Sci. (including Subser. Lect. Notes Artif. Intell. Lect. Notes Bioinformatics), 1935 (2000) 50–61.

[100] D.W. Shattuck, M. Mirza, V. Adisetiyo, C. Hojatkashani, G. Salamon, K.L. Narr, R.A. Poldrack, R.M. Bilder and A.W. Toga, *Construction of a 3D probabilistic atlas of human cortical structures*, Neuroimage, 39(3) (2008) 1064–1080.

[101] D.W. Shattuck, S.R. Sandor-Leahy, K.A. Schaper, D.A. Rottenberg and R.M. Leahy, *Magnetic resonance image tissue classification using a partial volume model*, Neuroimage 13(5) (2001) 856–876.

[102] E. Shelhamer, J. Long and T. Darrell, *Fully convolutional networks for semantic segmentation*, IEEE Trans. Pattern Anal. Mach. Intell., 39(4) (2017) 640–651.

[103] F. Shi, L. Wang, Y. Dai, J.H. Gilmore, W. Lin and D. Shen, *LABEL: Pediatric brain extraction using learning-based meta-algorithm*, Neuroimage 62(3) (2012) 1975–1986.

[104] S.M. Smith, *Fast robust automated brain extraction*, Hum. Brain Mapp. 17(3) (2002) 143–155.

[105] K. Somasundaram and K. Ezhilarasan, *Automatic brain portion segmentation from magnetic resonance images of head scans using gray scale transformation and morphological operations*, J. Comput. Assist. Tomogr. 39(4) (2015) 552–558.

[106] K. Somasundaram and T. Kalaiselvi, *Fully automatic brain extraction algorithm for axial T2-weighted magnetic resonance images*, Comput. Biol. Med. 40(10) (2010) 811–822.

[107] K. Somasundaram and T. Kalaiselvi, *Automatic brain extraction methods for T1 magnetic resonance images using region labeling and morphological operations*, Comput. Biol. Med. 41(8) (2011) 716–725.

[108] K. Somasundaram and R.S. Shankar, *Skull stripping of MRI using clustering and 2D region growing method*, Image Process, NCIMP (2010) 133–135.

[109] W. Speier, J.E. Iglesias, L. El-Kara, Z. Tu and C. Arnold, *Robust skull stripping of clinical glioblastoma multiforme data*, Int. Conf. Med. Image Comput. Computer-Assisted Interven. 14(pt3) (2011) 659–666.

[110] K. Srinivasan and N.M. Nanditha, *An intelligent skull stripping algorithm for MRI image sequences using mathematical morphology*, Biomed. Res. 29(16) (2018) 3201–3206.

[111] J.S. Suri, *Two-dimensional fast magnetic resonance brain segmentation*, IEEE Eng. Med. Biol. Mag. 20(4) (2001) 84–95.

[112] D.P. Waber, C.D. Moor, P.W. Forbes, C.R. Almli, K.N. Botteron, G. Leonard, D. Milovan, T. Paus, J. Rumsey and Brain Development Cooperative Group, *The NIH MRI study of normal brain development: Performance of a population based sample of healthy children aged 6 to 18 years on a neuropsychological battery*, J. Int. Neuropsychol. Soc. 13(5) (2007) 729–746.

[113] L. Wang, Y. Chen, X. Pan, X. Hong and D. Xia, *Level set segmentation of brain magnetic resonance images based on local gaussian distribution fitting energy*, J. Neurosci. Methods, 188(2) (2010) 316–325.

[114] Y. Wang, J. Nie, P.T. Yap, F. Shi, L. Guo and D. Shen, *Robust deformable-surface-based skull-stripping for large-scale studies yaping*, Lect. Notes Comput. Sci. (including Subser. Lect. Notes Artif. Intell. Lect. Notes Bioinformatics) 6893(3) (2011) 635–642.

[115] S. Wang, Y. Shi, H. Zhuang, C. Qin and W. Li, *Anatomical skull-stripping template and improved boundary-oriented quantitative segmentation evaluation metrics*, J. Med Imaging Heal. Inf. 10 (2020) 693–704.

[116] J. Wang, Z. Sun, H. Ji, X. Zhang, T. Wang and Y. Shen, *A fast 3D brain extraction and visualization framework using active contour and modern OpenGL pipelines*, IEEE Access 7 (2019) 156097–156109.

[117] B.D. Ward, *Intracranial segmentation*, Biophys. Res. Institute, Med. Coll. Wisconsin, (1999).

[118] B. Yilmaz, A. Durdu and G.D. Emlik, *A new method for skull stripping in brain MRI using multistable cellular neural networks*, Neural Comput. Appl. 29(8) (2018) 79–95.

[119] L. Yu, J.Z. Cheng, Q. Dou, X. Yang, H. Chen, J. Qin and P.A. Heng, *Automatic 3D cardiovascular MR segmentation with densely-connected volumetric ConvNets*, Lect. Notes Comput. Sci. (including Subser. Lect. Notes Artif. Intell. Lect. Notes Bioinformatics), 10434 (2017) 287–295.

[120] W. Zhang R. Li, H. Deng, L. Wang, W. Lin, S. Ji and D. Shen, *Deep convolutional neural networks for multi-modality isointense infant brain image segmentation*, Neuroimage 108 (2015) 214–224.

[121] Q. Zhang, L. Wang, X. Zong, W. Lin, G. Li and D. Shen, *FRNET: Flattened residual network for infant MRI skull stripping*, Proc. Int. Symp. Biomed. Imag. 2019 (2019) 999–1002.

[122] A.H. Zhuang, D.J. Valentino and A.W. Toga, *Skull-stripping magnetic resonance brain images using a model-based level set*, Neuroimage 32(1) (2006) 79–92.